Theory of $K\alpha$ generation by femtosecond laser-produced hot electrons in thin foils

D. Salzmann,* Ch. Reich, I. Uschmann, and E. Förster
Abteilung Röntgenoptik, Institut für Optik und Quantenelektronik, Friedrich-Schiller-Universität Jena, Max-Wien-Platz 1, D-07743 Jena, Germany

P. Gibbon
Central Institute for Applied Mathematics, Research Center Jülich, D-52425 Jülich, Germany
(Received 10 August 2001; published 8 February 2002)

An analytical model of femtosecond $K\alpha$ x-ray generation from laser-irradiated foils is presented. Expressions are found for the photon emission yield in both forward and backward directions in integral form as a function of hot-electron temperature and target thickness. It is found that for any given target material, there is a foil thickness and a hot-electron temperature at which the $K\alpha$ emission is maximized. Conversion efficiencies are consistent with contemporary measurements of $K\alpha$ radiation produced with femtosecond lasers.

DOI: 10.1103/PhysRevE.65.036402 PACS number(s): 52.25.−b, 52.65.Rr

I. INTRODUCTION

Recently published results, in which hard x rays from laser-produced plasmas were used to detect the melting of crystalline solids on the femtosecond time scale, have pushed the technique of time-resolved x-ray diffraction to the forefront of ultrafast science [1–4]. These pioneering experiments, which combine the femtosecond time-resolution offered by state-of-the-art lasers with subatomic spatial resolution, go a long way to realizing the early potential demonstrated by subpicosecond laser-plasma interaction as a means of creating x-ray flash lamps [5–8].

These early studies made little distinction between soft x rays from the cooling laser-generated plasma, and hard *K*-shell line radiation from the cold (unionised) material behind the surface plasma layer. However, it is hard (multi-keV) x rays that are of primary interest in the new fields of ultrafast x-ray diffractometry and biomedical radiography (x-ray imaging). These x rays are produced by energetic electrons created at the surface of the target irradiated by an intense laser pulse. Depending on their energy and the target material (Z), the electrons will typically penetrate several microns into the solid, generating bremsstrahlung and $K\alpha$ line radiation as they slow down via collisions with cold atoms. The characteristic $K\alpha$ radiation has received most attention to date because of its above-mentioned potential as a monoenergetic, pulsed, and high-brightness x-ray source. It is thus natural to ask how many hard x rays are produced by this means; a question whose solution involves several stages: the efficiency with which the laser energy is converted to hot electrons; the rate at which the electrons are slowed down and scattered in the solid; and the efficiency with which x-ray photons are generated by an electron.

A recent study by the Jena group found that for fixed laser energy, there is an optimum electron energy (or equivalently, laser intensity) to generate $K\alpha$ photons in material of a given atomic number Z [9]. This effect was attributed to self-absorption of the $K\alpha$ photons: x rays generated deep inside the target by very energetic electrons are absorbed before they can reach the surface, and so are not detected. This effect has also been observed in experiments where the position of the laser focus was varied along the target normal [10]. The purpose of this paper is to formulate a general *space-dependent* model in which the photon reabsorption is included self-consistently, and does not rely on empirical input from numerical simulation [9]. As we will see later, this model allows us to explore the interplay between the three length scales: electron stopping range, target thickness, and photon mean free path.

The paper is organized as follows: in Sec. II we derive a general formula for the $K\alpha$ yield from a laser-irradiated slab in both the forward and backward directions; in Sec. III this model is used to determine optimal conditions for $K\alpha$ emission by finding the dependence on target and hot-electron characteristics. In particular, a relationship between the target thickness and the electron energy is found that provides the maximum $K\alpha$ yield. In Sec. IV these results are then generalized for a range of target materials.

II. MODEL OF $K\alpha$ GENERATION IN SLAB TARGETS OF FINITE WIDTH

First we suppose that the laser has created a population of hot electrons on the ''front'' side of the target and that these are directed into the slab along the target normal. This assumption is reasonable for nonrelativistic electrons, regardless of the angle of incidence of the laser; for relativistic kinetic energies, the penetration angle becomes energy dependent [11–13]. Recent experiments [11,14] with short-pulse lasers indicate that the electron energy distribution has an exponential high-energy tail of the form

$$f(E) = \frac{1}{T_h}\exp(-E/T_h), \tag{1}$$

where T_h is the hot-electron temperature in keV. The latter may be related to the laser irradiance $I\lambda^2$ if the absorption mechanism is known, but we defer discussion of this point

*On sabbatical leave from Department of Applied Physics, Soreq NRC, Yavne 81800, Israel.

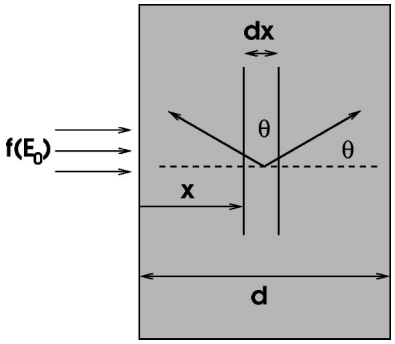

FIG. 1. Geometry of $K\alpha$ emission from a one-dimensional slab target.

until later. Consider then, the $K\alpha$ emission due to a distribution of N_h hot electrons passing through a slab of thickness d, as depicted in Fig. 1. Up to electron energies of about 100 keV, the stopping power of any target material can be approximated to high accuracy by [15]

$$\frac{dE}{dx}=AE^{-\alpha}, \quad \alpha>0, \tag{2}$$

where A and α are Z-dependent constants. Above 100 keV, the stopping power shows significant deviation from this simple form, mainly due to relativistic effects. The initial energy of the electron E_0 and its energy E at depth x, are connected by the integral equation,

$$x=\int_0^x dx=\int_E^{E_0}\frac{dE}{dE/dx}. \tag{3}$$

In the region where Eq. (2) is valid, this reduces to a rather simple relationship,

$$x=\frac{1}{(1+\alpha)A}(E_0^{\alpha+1}-E^{\alpha+1}). \tag{4}$$

At higher energies, there is no simple analytical solution to Eq. (3).

The number of $K\alpha$ photons generated by electrons with energies E within the interval $[x,x+dx]$ emitted into a solid angle Ω_D at an angle θ relative to the electron penetration axis is given by

$$dN_{K\alpha}=N_h f[E_0(E,x)]dE\,\omega_K n_A \sigma_K(E)dx\frac{\Omega_D}{4\pi}$$
$$\times\begin{cases}\exp(-n_A\sigma_{ph}x/|\cos\theta|) & \text{for } \dfrac{\pi}{2}<\theta\leqslant\pi,\\ \exp(-n_A\sigma_{ph}(d-x)/|\cos\theta|) & \text{for } 0<\theta\leqslant\dfrac{\pi}{2},\end{cases} \tag{5}$$

where $\sigma_K(Z,E),\omega_K(Z),n_A(Z)$, and $\sigma_{ph}(Z,h\nu_K)$ are, respectively, the cross section for K-shell ionization; the $K\alpha$ fluorescence yield; the atomic number density; and the photoabsorption cross section for a $K\alpha$ photon. The argument of f $[\cdots]$ reflects the fact that electrons with energy E at depth x *started off* with energies of $E_0(E,x)$ when they entered the target, where $E_0(E,x)$ is the solution of Eq. (3) for a given E and x. Expression (5) also assumes that electrons travel in a straight line, that is, elastic scattering is neglected. The effect of scattering is to reduce the effective penetration depth of electrons for a given stopping range or initial energy E_0. The relationship between E,x, and E_0 becomes more complex, so we defer quantitative consideration of this effect until Sec. III. Defining an angle-dependent photon mean free path,

$$\lambda_{\rm mfp}(\theta)=\frac{|\cos\theta|}{n_A\sigma_{ph}(h\nu_K)},$$

and integrating, we have:

$$N_{K\alpha}=N_h n_A\omega_K\frac{\Omega_D}{4\pi}\int_0^\infty dE\,\sigma_K(E)\int_0^d dx f[E_0(E,x)]$$
$$\times\begin{cases}\exp\left(-\dfrac{x}{\lambda_{\rm mfp}}\right) & \text{backward},\\ \exp\left(-\dfrac{d-x}{\lambda_{\rm mfp}}\right) & \text{forward}.\end{cases} \tag{6}$$

We note that the two integrals in Eq. (6) cannot be performed independently because of the x dependence of the electron energy loss $\Delta E(x)=E_0-E$. Nonetheless, we can make some progress by exploiting the exponential form of the hot-electron distribution in Eq. (1). We first define the dimensionless quantities $Q_\pm$ by

$$Q_+(E)=\int_0^d\frac{dx}{\lambda_{\rm mfp}}\exp\left(-\frac{E_0(E,x)}{T_h}\right)\exp\left(-\frac{d-x}{\lambda_{\rm mfp}}\right),$$

$$Q_-(E)=\int_0^d\frac{dx}{\lambda_{\rm mfp}}\exp\left(-\frac{E_0(E,x)}{T_h}\right)\exp\left(-\frac{x}{\lambda_{\rm mfp}}\right). \tag{7}$$

Substituting $y=x/\lambda_{\rm mfp}$ and $\xi_d=d/\lambda_{\rm mfp}$, this is reduced to

$$Q_+(E)=\int_0^{\xi_d}dy\exp\left(-\left[\frac{E_0(E,y\lambda_{\rm mfp})}{T_h}+\xi_d-y\right]\right), \tag{8}$$

and for the backward x rays

$$Q_-(E)=\int_0^{\xi_d}dy\exp\left(-\left[\frac{E_0(E,y\lambda_{\rm mfp})}{T_h}+y\right]\right). \tag{9}$$

Equation (6) then takes the form

$$N_{K\alpha}=N_h n_A\omega_K\frac{\Omega_D}{4\pi}\frac{\lambda_{\rm mfp}}{T_h}\int_0^\infty dE\,\sigma_K(E)Q_\pm(E). \tag{10}$$

Equation (10) together with Eqs. (8) and (9) represents the most general form of $K\alpha$ emission from a finite, one-dimensional (1D) slab. It is helpful to recast these three equations in terms of the average $K\alpha$ emission *efficiency* ε_f

defined as the number of $K\alpha$ photons emitted per hot electron per steradian. This is obtained simply by dividing Eq. (10) by Ω_D and N_h,

$$\varepsilon_f = \frac{1}{4\pi} n_A \omega_K \frac{\lambda_{\mathrm{mfp}}}{T_h} \int_0^\infty dE \sigma_K(E) Q_\pm(E). \tag{11}$$

The advantage of this definition is that ε_f is independent of various experimental factors: the detector system (which typically encompasses a small, finite solid angle); the generally complex variation of N_h with laser parameters; and the shape of the laser pulse and/or possible prepulses, which influence the fractional energy dump into hot electrons. We shall, however, return to some of these points later in the paper.

The numerical method used to solve Eq. (11) consists of three steps: (i) first, a matrix of E_0's is obtained from Eq. (3) on a logarithmic 2D mesh of E's and x's. By means of this matrix, given that an electron has energy E at depth x, one can reconstruct the energy it had at the target surface via interpolation. (ii) Using this matrix, the values of $Q_\pm(E)$ can be computed on a mesh of energies. (iii) Finally, the integration over the energy E is carried out using Simpson's rule, interpolating $Q_\pm(E)$ between the energy mesh points. The overall accuracy of the integration is better than a few percent.

We now proceed to analyze these equations with the aim of finding optimal conditions for emission as a function of target thickness, electron energy (or laser intensity), and target material. In the calculations that follow, the stopping power was taken from Ref. [15]; the $K\alpha$ emission cross sections, σ_K from Ref. [16]; the fluorescence yields, ω_K from Ref. [17]. The effect of screening on the atomic states is also included in Refs. [15] and [16]. To the best of our knowledge, these databases have the highest available accuracy to date. It should be noted, however, that the fluorescence yields in Ref. [17] refer to solid state cold material. For compressed plasmas, the collision rates may become comparable with the $L \rightarrow K$ radiative emission rate. At such densities the fluorescence yields have to be modified due to collisions, and one should then adopt a generalized collisional-radiative model to account for the collisional effects. A computational study of these effects was carried out in Ref. [18]. Their results reduce to the vacancy-cascade fluorescence yields in Ref. [17] at the lower densities of our targets.

III. TARGET THICKNESS AND HOT-ELECTRON TEMPERATURE

Unlike the semiempirical model of Ref. [9], the present model treats the spatial dependence of the $K\alpha$ generation and reabsorption explicitly, and does not rely on any averaging over the emission region. Thus, we may determine the variation of the photon yield from the thin foil ($d < \lambda_{\mathrm{mfp}}$) to the thick target limit ($d \gg \lambda_{\mathrm{mfp}}$). An example of this is shown in Fig. 2, which shows the $K\alpha$ yield in both forward and backward directions calculated from Eq. (10) for titanium foils of varying thicknesses and laser parameters consistent with hot-electron temperatures $T_h = 10$ keV–150 keV. The

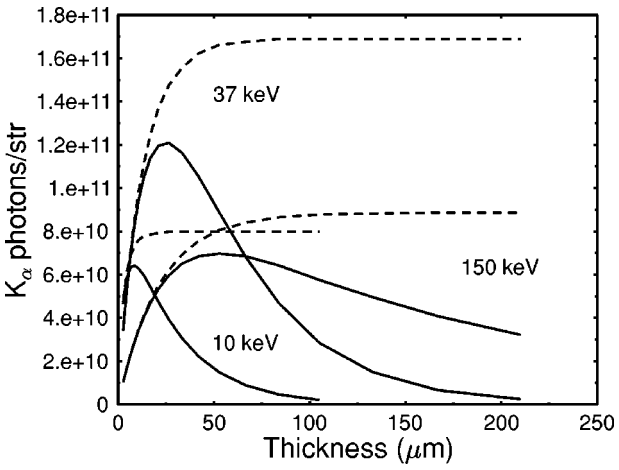

FIG. 2. Dependence of forward (solid lines) and backward (dashed lines) $K\alpha$ emission on foil thickness for a Ti target bombarded by hot electrons with three different temperatures. The forward/backward emission curves merge for very thin foils.

thick-target limit for backward emission (i.e., photons detected on the ''frontside'' of the target where the laser is incident) is recovered in this case for thicknesses above 100 μm (saturated part of the curve). This value is comparable with the one obtained from Eq. (5) in Ref. [9], after appropriate scaling of laser parameters. Clearly there is an overall optimal thickness—about 25 μm for $T_{hot} = 37$ keV—for emission in the forward direction (rear-side of target), when the thickness matches the photon mean free path, $\lambda_{mfp} = 26.5$ μm. Similar curves are obtained for other materials too, such as aluminum ($Z = 13$), copper ($Z = 29$), molybdenum ($Z = 42$), erbium ($Z = 68$), and gold ($Z = 79$), after making appropriate changes in foil thickness and hot-electron temperature. As noted earlier, we expect elastic scattering to reduce these optimal values. To find out by how much, the curve for 37 keV was recomputed by using a full Monte Carlo calculation [9] in place of Eq. (3) to obtain the matrix $E_0(E,x)$. The latter actually becomes multivalued, exhibiting a spread of initial electron energies for each penetration depth; however, the mean can still be fed into Eq. (11) to estimate the average $K\alpha$ production efficiency. Comparing the result of this more complex calculation with the simple stopping model used here, we find that the efficiency is reduced by up to 20% and the optimal thickness by 30-40 % when elastic scattering is included. We conclude that scattering will make a similar quantitative, rather than qualitative difference to the other curves in Fig. 2, as well as for the other materials considered. For simplicity, therefore, we will henceforth stick to our original ''straight-line'' approximation, but bear in mind that the optimal thicknesses obtained may be systematically overestimated.

In this spirit we proceed to determine the optimal thicknesses for a *series* of hot-electron temperatures—Fig. 3. For the backward emission, this thickness is defined as the value where the emission reaches 80% of its saturation value in the thick-target limit ($d = \infty$). This somewhat arbitrary-sounding choice is motivated by the need to minimize background radiation and to eliminate the ''afterglow'' created by highly

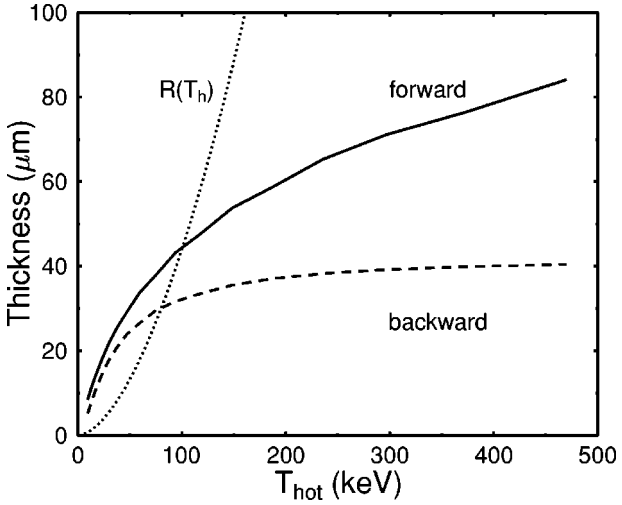

FIG. 3. Foil thickness required to maximize forward (solid line) and backward (dashed line) $K\alpha$ emission as a function of hot-electron temperature for a titanium target.

energetic electrons [9]. Also shown on this plot is the electron range estimated from Eq. (4) for a monoenergetic beam with energy equal to T_h.

Common sense leads us to expect maximum conversion efficiency when the target thickness exceeds the electron stopping distance; that is, for electron energies of around 100 keV in this case. This is confirmed in Fig. 4(a), which shows the $K\alpha$ efficiencies ε_f corresponding to the optimal foil thickness at a given hot-electron temperature $d_{opt}(T_h)$—Fig. 3.

Of more practical interest, however, are the curves in Fig. 4(b), that are obtained by multiplying the efficiencies by the number of hot electrons N_h. Imposing a constraint that the laser energy absorbed by hot electrons, $U_a = \eta U_L \simeq N_h T_h$ is constant, this effectively means dividing ε_f by T_h. In this example, we took a total laser energy, $E_L = 1$ J, pulse duration $\tau_L = 100$ fs and absorption fraction $\eta = 10\%$ into hot electrons. We thus end up with both an optimal thickness *and* hot-electron temperature for a given laser energy and target material. Note that the optimal T_h is the same for $K\alpha$ radiation emitted in both forward and backward directions, even though the optimal thickness for backscattered radiation is infinite.

IV. *Z* DEPENDENCE

A curious outcome of the thick-target model in Ref. [9] was that there appeared to be a universal optimal hot-electron temperature, T_h for $K\alpha$ generation, equal to about six times the *K*-shell ionization energy E_K, which was *independent* of *Z*. This universality can be traced to the approximate manner in which the effect of photon absorption was included, i.e., by introducing an ''emission factor'' whereby electrons with energies beyond a fixed multiple of E_K produced photons too deep into the target to be detected. The present model contains no such simplification, so it is naturally of interest to see whether this behavior is reproduced when absorption is taken into account self-consistently. The

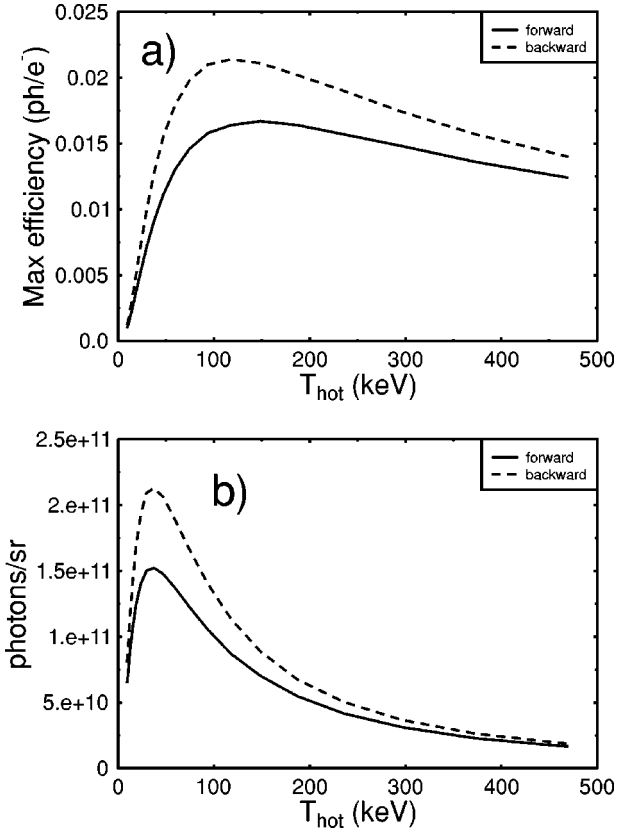

FIG. 4. (a) Photon efficiency and (b) photon yield for constant laser energy and optimum target thickness as a function of hot-electron temperature for a titanium target.

result is displayed in Fig. 5, which shows that the required ratio of T_h to the *K*-shell energy does in fact depend weakly on *Z*. We see that the ratio varies from around 12 (aluminum, $Z = 13$) to 4 for high-*Z* targets (gold, $Z = 79$). The value of $T_h/E_K \simeq 6$ obtained by Reich *et al.* is, therefore, a reasonable average, given that the $K\alpha$ emission shows a fairly broad resonance about this optimum. On the other hand, it is possible that the *Z* dependence exhibited by our model might be diluted by elastic scattering: however, to determine whether

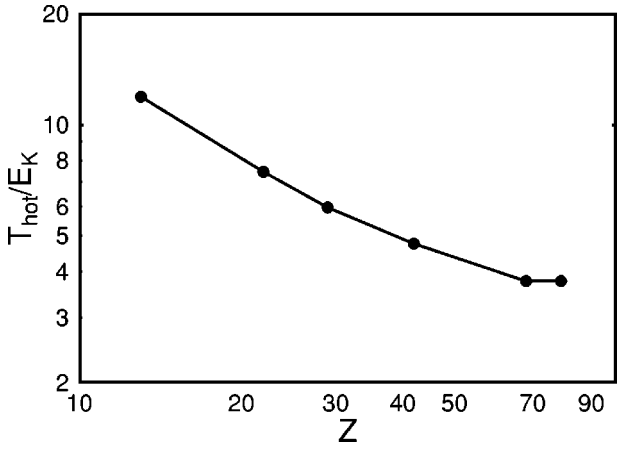

FIG. 5. Optimal ratio of hot-electron temperature to *K*-shell ionization energy for different target materials *Z*.

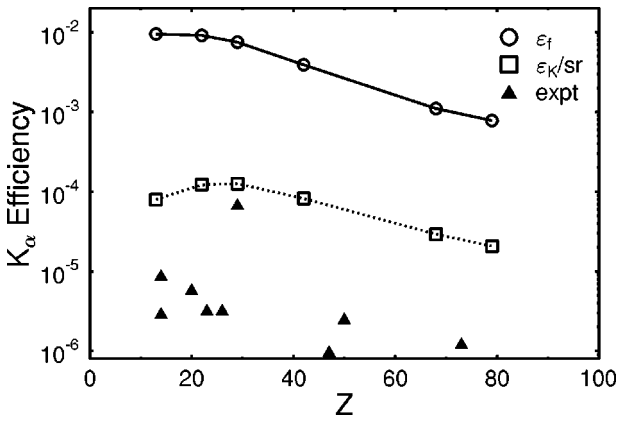

FIG. 6. $K\alpha$ production efficiencies under optimal conditions for various target materials Z: photons per electron (circles); energy conversion efficiency per steradian (squares) and experimental measurements (filled triangles—see text).

this is the case would involve several hundred Monte Carlo calculations, a task well beyond the scope of the present paper.

For experimental purposes it is of course useful to know how many $K\alpha$ photons can be expected for a given target material under optimized conditions. This is shown in Fig. 6, which assumes all other parameters—T_h and d have been optimized. Here we plot both ε_f defined according to Eq. (11), and the overall conversion efficiency ε_K from the laser into the $K\alpha$ x-ray line *per steradian*. To get the latter, we use the following relation:

$$\varepsilon_K = \varepsilon_f \frac{N_h E_{K\alpha}}{U_L} = \varepsilon_f \eta \frac{E_{K\alpha}}{T_h}, \tag{12}$$

where $E_{K\alpha}$ is the $K\alpha$ photon energy and we have again assumed that the absorbed laser energy is fixed: $N_h T_h = \eta U_L$. As in Fig. 4, we take $\eta = 10\%$ and $U_L = 1$ J in this example: this gives a representative estimate of the maximum possible conversion efficiency that can be expected for typical laser parameters. For comparison, a number of experimentally measured values are shown too, taken from the following sources: Soom *et al.* [19], Bastiani *et al.* [20] ($Z=14$); Rousse *et al.* [8] ($Z=13,20,26$); Jiang *et al.* [21] ($Z=23$); Eder *et al.* [10] (29); Yu *et al.* [22] ($Z=47$); Andersson *et al.* [23] ($Z=50,73$). These data generally fall well below the theoretical curves, which suggests that the experimental conditions —here consisting of a variety of laser intensities and target thicknesses—were far from optimal for $K\alpha$ generation.

V. CONCLUSIONS

In summary, we have formulated a general model of $K\alpha$ generation in femtosecond laser-irradiated solid material. Photon reabsorption is taken into account explicitly, permitting both forward and backscattered emission to be calculated for arbitrary target thicknesses. It is found that there is both an optimal target thickness and hot-electron temperature for forward emission, at which point the thickness, electron range, and mean free path of the $K\alpha$ photons are roughly equal. This temperature varies between 4 and 12 times the K-shell ionization energy, depending on the atomic number; a result that is consistent with the ''universal'' optimal ratio $T_h/E_K \simeq 6$ found previously by Reich *et al.* [9]. Comparison of the photon conversion efficiencies expected from the model with recent measurements suggests that experimental conditions (laser and target parameters) could probably be better matched in order to enhance the $K\alpha$ yield. The model may thus serve as a guide for application experiments using both backward and forward emission geometries.

ACKNOWLEDGMENT

This work was supported in part by the Deutsche Forschungsgemeinschaft, Contract No. GI-300/2.

[1] C. Rischel *et al.*, Nature (London) **390**, 490 (1997).
[2] C.W. Siders *et al.*, Science **286**, 1340 (1999).
[3] T. Feurer *et al.*, Appl. Phys. B: Lasers Chem. **72**, 15 (2001).
[4] A. Rousse *et al.*, Nature (London) **410**, 65 (2001).
[5] D.G. Stearns, O.L. Landen, E.M. Campbell, and J.H. Scofield, Phys. Rev. A **37**, 1684 (1988).
[6] D. Kuhlke, U. Herpes, and D. von der Linde, Appl. Phys. Lett. **50**, 1785 (1987).
[7] J.C. Kieffer *et al.*, Phys. Fluids B **5**, 2676 (1993).
[8] A. Rousse *et al.*, Phys. Rev. E **50**, 2200 (1994).
[9] Ch. Reich, P. Gibbon, I. Uschmann, and E. Förster, Phys. Rev. Lett., **84**, 4846 (2000); Laser Part. Beams **19**, 147 (2001).
[10] D.C. Eder *et al.*, Appl. Phys. B: Lasers Opt. **70**, 211 (2000).
[11] H. Schwoerer *et al.*, Phys. Rev. Lett. **86**, 2317 (2001).
[12] A.A. Andreev, I.A. Litvinenko, and K.Y. Platonov, Pis'ma Zh. Eksp. Teor. Fiz. **116**, 1184 (1999) [JETP Lett. **89**, 632 (1999)].
[13] Z.-M. Sheng *et al.*, Phys. Rev. Lett. **85**, 5340 (2000).
[14] G. Malka and J.L. Miquel, Phys. Rev. Lett. **77**, 75 (1996).
[15] S. T. Perkins, D. E. Cullen, and S. M. Seltzer, Technical Report No. UCRL-50400, LLNL (unpublished).
[16] C. Hombourger, J. Phys. B **31**, 3693 (1998).
[17] W. Bambynek *et al.*, Rev. Mod. Phys. **44**, 716 (1972).
[18] V.L. Jacobs *et al.*, Phys. Rev. A **21**, 1917 (1980); V.L. Jacobs and B.F. Rosznyai, *ibid.* **34**, 216 (1986).
[19] B. Soom, H. Chen, Y. Fisher, and D.D. Meyerhofer, J. Appl. Phys. **74**, 5372 (1993).
[20] S. Bastiani *et al.*, Phys. Rev. E **56**, 7179 (1997).
[21] Z. Jiang *et al.*, Phys. Plasmas **2**, 1702 (1995).
[22] J. Yu, Z. Jiang, J.C. Kieffer, and A. Krol, Phys. Plasmas **6**, 1318 (1999).
[23] E. Andersson *et al.*, J. Appl. Phys. **90**, 3048 (2001).